Am J Physiol Cell Physiol 299: C1504–C1515, 2010.
First published September 29, 2010; doi:10.1152/ajpcell.00015.2010.

Connexin 43 hemichannels mediate the Ca^{2+} influx induced by extracellular alkalinization

Kurt A. Schalper,[1] Helmuth A. Sánchez,[1] Sung C. Lee,[2] Guillermo A. Altenberg,[2] Michael H. Nathanson,[3] and Juan C. Sáez[1,4]

[1]*Departamento de Ciencias Fisiológicas, Pontificia Universidad Católica de Chile, Santiago, Chile;* [2]*Department of Cell Physiology and Molecular Biophysics, and Center for Membrane Protein Research, Texas Tech Health Sciences Center, Lubbock Texas;* [3]*Department of Internal Medicine, Yale University School of Medicine, New Haven, Connecticut; and* [4]*Núcleo Milenio de Inmunología e Inmunoterapia, Santiago, Chile*

Submitted 13 January 2010; accepted in final form 16 September 2010

Schalper KA, Sánchez HA, Lee SC , Altenberg GA, Nathanson MH, Sáez JC. Connexin 43 hemichannels mediate the Ca^{2+} influx induced by extracellular alkalinization. *Am J Physiol Cell Physiol* 299: C1504–C1515, 2010. First published September 29, 2010; doi:10.1152/ajpcell.00015.2010.—Although alkaline pH is known to trigger Ca^{2+} influx in diverse cells, no pH-sensitive Ca^{2+} channel has been identified. Here, we report that extracellular alkalinization induces opening of connexin 43 hemichannels (Cx43 HCs). Increasing extracellular pH from 7.4 to 8.5, in the presence of physiological Ca^{2+}/Mg^{2+} concentrations, rapidly increased the ethidium uptake rate and open probability of HCs in Cx43 and Cx43EGFP HeLa transfectants (HeLa-Cx3 and HeLa-Cx43EGFP, respectively) but not in parental HeLa cells (HeLa-parental) lacking Cx43 HCs. The increase in ethidium uptake induced by pH 8.5 was not affected by raising the extracellular Ca^{2+} concentration from 1.8 to 10 mM but was inhibited by a connexin HC inhibitor (La^{3+}). Probenecid, a pannexin HC blocker, had no effect. Extracellular alkalinization increased the intracellular Ca^{2+} levels only in cells expressing HCs. The above changes induced by extracellular alkalinization did not change the cellular distribution of Cx43, suggesting that HC activation occurs through a gating mechanism. Experiments on cells expressing a COOH-terminal truncated Cx43 mutant indicated that the effects of alkalinization on intracellular Ca^{2+} and ethidium uptake did not depend on the Cx43 C terminus. Moreover, purified dephosphorylated Cx43 HCs reconstituted in liposomes were Ca^{2+} permeable, suggesting that Ca^{2+} influx through Cx43 HCs could account for the elevation in intracellular Ca^{2+} elicited by extracellular alkalinization. These studies identify a membrane pathway for Ca^{2+} influx and provide a potential explanation for the activation of cellular events induced by extracellular alkalinization.

alkaline pH; liposomes; connexons; calcium permeability

PLASMA MEMBRANE Ca^{2+} CHANNELS are ubiquitous and serve an essential role in the regulation of varied cell processes such as muscle contraction, neurotransmitter release, epithelial secretion, maintenance of cell volume, and cell proliferation and migration (19, 36, 43). Three types of plasma membrane Ca^{2+} channels have been identified: voltage-gated, ligand-gated, and store-operated channels. However, the membrane pathway of the increased Ca^{2+} influx induced by alkaline extracellular pH has not been identified.

Connexin hemichannels (Cx HCs) are functional membrane hexameric channels present in diverse primary cell types such as astrocytes (11), myocardiocytes (30), kidney epithelial cells (70), osteocytes (10), hepatocytes (72), and neurons (63), as well as in cell lines derived from fibroblasts (24), endothelial cells (23), osteoblasts (57), and monocytes/macrophages (74), among others. Recent studies (22, 25, 26, 32, 41, 47) also support the presence of functional Cx HCs in tissues where they play relevant functions. Undocked HCs correspond structurally to half a gap junction channel, but instead of being at apposed cell membranes, as gap junction channels are (22), they are located at unapposed cell membrane domains and frequently show independent regulation and function from those of intercellular channels (11, 14, 22, 54, 60). Although HCs are believed to remain preferentially closed in cultured cells under resting conditions (4), their activation has been documented under experimental conditions of different physiological and pathophysiological natures (22, 60, 62). Hemichannels formed by connexin43 (Cx43), the most ubiquitous gap junction protein, participate in diverse cellular processes by mediating the transmembrane passage of small molecules such as ATP (32), NAD^+ (7), glutamate (75), glutathione (51), PGE_2 (10), and glucose (54).

A single channel conductance of ~220 pS is characteristic of Cx43 HCs activated by positive membrane voltages (12) or by extracellular ligands such as proinflammatory cytokines (54) and FGF-1 (60), which increase their open probability. The predicted Cx43 HC pore diameter is rather large (68), and as expected, these HCs constitute nonselective pathways for ions and are permeable to molecules larger and more complex than small inorganic ions (22, 61, 37, 38). In theory, Ca^{2+} permeation through Cx43 HCs could explain their involvement in several physiological and pathological responses associated with HC activation (11, 14, 15, 24, 25, 26, 30, 38, 44, 47, 50, 58, 60). However, extracellular divalent cations such as Ca^{2+} and Mg^{2+} reduce the open probability of Cx HCs (18, 37, 67), and the open probability of all Cx HCs so far studied is rapidly enhanced by removal of extracellular divalent cations (22, 37, 60). Although the blocking effect of divalent cations may prevent or limit Ca^{2+} fluxes through HCs, the divalent cation effect seems to be overcome under certain circumstances. For example, under resting conditions, physiological extracellular Ca^{2+} concentration ($[Ca^{2+}]$) reduce the open probability of Cx43 HCs (12), limiting Ca^{2+} inflow. However, Cx43 HC activation occurs in the presence of extracellular divalent cations under conditions that mimic ischemic, proinflammatory, or proliferative conditions (11, 14, 15, 24, 26, 30, 34, 47, 54, 60, 65) or treatment with nitric oxide donors (52) or reducing agents (53). Exposure of rabbit cardiomyocytes to metabolic inhibitors for 60 min increases the intracellular

Address for reprint requests and other correspondence: K. A. Schalper, Departamento de Fisiología, Pontificia Universidad Católica de Chile, Alameda 340, 4 to Piso, Santiago, 8331150 Chile (e-mail: kschalpe@med.puc.cl).

 0363-6143/10 Copyright © 2010 the American Physiological Society

[Na^+] and [Ca^{2+}], effects reduced ~50% by the nonselective HC and gap junction blockers halothane and heptanol (38). Furthermore, the increase in intracellular [Ca^{2+}] in isolated rat neonatal cardiomyocytes exposed to oxygen and glucose deprivation is inhibited by Gap26, a Cx mimetic peptide blocker of Cx43 HCs (65). The above results suggest the occurrence of Ca^{2+} influx via HCs. However, after metabolic stress, intracellular Na^+ accumulation reduces the Ca^{2+} efflux through Na^+/Ca^{2+} exchange and also via plasma membrane Ca^{2+}-ATPase (PMCA), promoting intracellular Ca^{2+} accumulation (9). In addition, dantrolene, a blocker of Ca^{2+} release from endoplasmic reticulum also inhibits the elevation in intracellular [Ca^{2+}] induced by ischemic-like conditions (65). Therefore, a role of Ca^{2+} influx through activated HCs is possible but remains uncertain.

In Cx43 HeLa transfectants treated with FGF-1 or 4Br-A23187, a Ca^{2+} ionophore, cell permeabilization is directly related to an increase in surface Cx43 levels (60). The FGF-1 effect requires and favors an increase in intracellular [Ca^{2+}], suggesting that Cx43 HCs are permeable to this ion (60). Although Ca^{2+} influx associated with HC expression is required for the metabolic inhibition-induced increase in surface HC levels, as well as for the resulting cell permeabilization to ethidium in HeLa cells transfected with Cx32 (58), there is no demonstration of Cx43 HC permeability to Ca^{2+} in cells exposed to alkaline pH.

Here, using HeLa transfectants, electrophysiological measurements, and confocal time-lapse fluorescence recordings, we show that HCs formed by Cx43 are activated by extracellular alkalinization. Our data strongly suggest that activated Cx43 HCs are permeable to Ca^{2+} and that the Cx43 COOH-terminal domain is not essential for sensing rises in extracellular pH.

MATERIALS AND METHODS

Reagents and solutions. We used a previously characterized polyclonal anti-Cx43 antibody (6, 60) and a monoclonal antibody against an epitope of the NH_2-terminal tail of mouse Cx43 (anti-NT1 antibody) generously provided by Dr. Paul Lampe (Fred Hutchinson Cancer Research Center, University of Washington, Seattle, WA; Ref. 66). An influenza hemagglutinin tag (cat. no. 71–5500) antibody was obtained from Zymed Laboratories (Carlsbad, CA). Ethidium bromide (Etd), $LaCl_3$ (La^{3+}), probenecid, and calf intestine alkaline phosphatase immobilized on agarose were obtained from Sigma-Aldrich (St. Louis, MO). Fluo 4-AM, fura red-AM, and calcium green-2 were from Invitrogen (Carlsbad, CA). The L-α-phosphatidylcholine and L-α-phosphatidylserine were purchased from Avanti Polar Lipids (Alabaster, Al), and the detergent *n*-decyl-β-D-maltopyranoside was from Antrace (Maumee, OH). The composition of the recording solution was as follows (in mM): NaCl (150), KCl (5.4), $CaCl_2$ (1.8), $MgCl_2$ (1), glucose (5), and HEPES (5), pH 7.4 or 8.5. The Etd used for dye uptake experiments was prepared in water and diluted to a 5 μM final concentration in recording solution. A 100 mM (100×) probenecid, stock solution was prepared in distilled water. $LaCl_3$ was dissolved in recording solution at 100× final concentration. All stock solutions were diluted to final concentrations in recording solution prepared in sterile and filtered water (W3500; Sigma-Aldrich).

HeLa cell cultures. Previously described parental HeLa cells (CCL-2; ATCC, Rockville, MD) and HeLa cells stably transfected with mouse Cx43 (HeLa-Cx43) were kindly provided by Dr. Klaus Willecke (Bonn University, Bonn, Germany; Ref. 20). A variant Cx43 truncated at amino acid 257 (Cx43Δ257) was generated by Dr. Agustín D. Martínez (Universidad de Valparaiso, Valparaiso, Chile) and was previously described by Schalper et al. (60). The vector used for Cx43 transfections was pcDNA1/Neo (Invitrogen), which contains the cytomegalovirus promoter, polyadenylation signal, and a gene conferring resistance to G418. The vector alone was transfected into HeLa cells to study the effect of transfection itself on the membrane permeability increase elicited by extracellular alkalinization. HeLa cells were transfected with 1 μg pcDNA I/Neo using the calcium phosphate transfection protocol. Twenty-four hours after removal of the DNA precipitate, G418 (300 μg/ml) was added to the culture medium. The transformed cells were resistant to G418 but did not express detectable levels of Cx43 (mock-transfected HeLa cells). HeLa cells expressing Cx43 with EGFP fused to its C terminus (HeLa-Cx43EGFP) were kindly provided by Dr. Feliksas Bukauskas (Albert Einstein College of Medicine, New York, NY) and have been described previously (8). Cells expressing Cx43Δ257 were selected with 300 μg/ml G418 and identified using an antibody directed against a 9 amino-acid influenza hemagglutinin tag inserted in the construct (60). All cells were cultured in DMEM supplemented with 10% FBS and kept at 37°C in a 5% CO_2/95% atmosphere at nearly 100% relative humidity. Cells expressing Cx43EGFP were selected with 300 μg/ml G418 and identified by their fluorescence emission at 530 nm, as described (60). Cells were seeded onto plastic Falcon Petri dishes (Becton Dickinson, Los Angeles, CA) or onto sterile glass coverslips placed on the bottom of plastic culture dishes. Cx expression was tested by indirect immunofluorescence (Fig. 1) or fluorescence intensity of the EGFP-tagged protein (Fig. 4). Cell cultures showing membrane staining in >95% of the cells were used in all experiments.

Extracellular alkalinization protocol. Extracellular alkalinization was achieved by superfusing cells with recording solution (see above) adjusted to pH 8.5 with NaOH/HCl. The pH of all solutions was titrated to the desired pH, at room temperature, and all solutions were prepared 30 min before each experiment. Subconfluent (<50%) and 48-h serum-starved HeLa cells were used since previous studies (60) revealed the highest HC-mediated response to FGF-1 under these conditions. Since relatively small extracellular osmolarity increases (e.g., 25 mosmol/l) activate Cx43 HCs in cardiomyocytes and Cx43-transfected HeLa cells (31), the osmolarity of control (pH 7.4) and alkaline solutions (pHs 7.8 and 8.5) was measured using a vapor pressure osmometer (Wescor 5520; Vapro, Logan, UT). As expected due to the low buffer concentration (5 mM HEPES), there was no significant difference between the osmolarity of the solutions (319 ± 5 mosmol/l at pH 7.4 vs. 323 ± 7 mosmol/l at pH 8.5; $P > 0.05$).

Time-lapse fluorescence imaging and intracellular [Ca^{2+}]. For time-lapse experiments, cells plated on glass coverslips were washed twice with recording solution and placed into a custom-made perfusion chamber on the stage of a Zeiss LSM 510 confocal microscope (Thornwood, NY), using a ×40 1.2 NA objective lens, essentially as described previously (56). Excitation was accomplished through the 488-nm line of a krypton/argon laser. In all cases, measurements and data analyses were performed using the same microscope and camera settings, at which neither autofluorescence nor background signals were detectable. Excitation intensity was low to prevent photobleaching, which was not observed when the cells were illuminated for a few minutes. For the Etd uptake experiments, cells were superfused with recording solution containing 1 μM Etd and fluorescence emission between 565 and 615 nm was recorded every 4 s in regions of interest of different cells. Results from 4–20 cells per experiment were averaged. For the assessment of cytosolic Ca^{2+} changes, cells were loaded for 45 min with the acetoxymethyl ester forms of fluo 4 (6 μM) or fura red (6 μM), at 37°C, followed by a 30-min deesterification period. After three washes in recording solution, cells were left to stabilize at 37°C for 5 min before recordings started. Emission was recorded between 500 and 530 nm for fluo 4, or above 650 nm for fura red, with acquisition rates of 1–5 Hz. Changes in fluorescence are presented as percentage of the difference between peak fluorescence and baseline fluorescence. In another set of time-lapse Etd uptake experi-

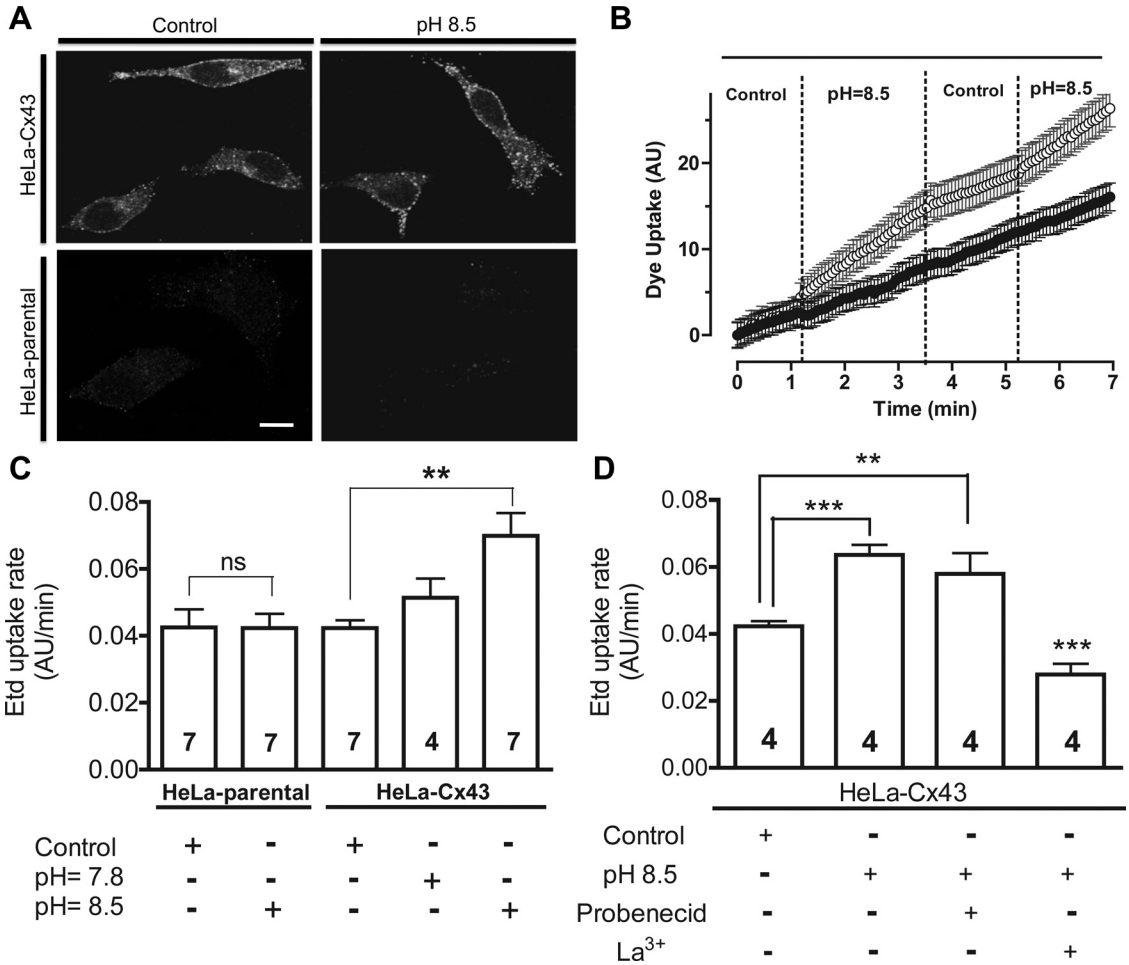

Fig. 1. Extracellular alkalinization increases the rate of ethidium (Etd) uptake in HeLa-connexin 43 (Cx43), but not in HeLa-parental cells, through Cx43 hemichannels (HCs), without changes in cellular distribution of Cx43. *A*: HeLa-Cx43 but not HeLa-parental cells showed Cx43 reactivity detected by immunofluorescence and confocal microscopy. Cx43 reactivity detected in cells incubated in control saline solution at pH 7.4 was comparable to that detected in cells incubated for 15 min in saline solution with pH 8.5. *B*: representative time-lapse experiments showing Etd uptake in HeLa-C43 (white circles) or HeLa-parental (black circles) under control condition (control, pH 7.4) and after extracellular alkalinization (pH 8.5). Data are means ± SE of 20 cells. Uptake was measured every 20 s as fluorescence emission intensity of Etd bound to DNA. Intensity is shown in arbitrary units (AU). *C*: Etd uptake rates of HeLa-parental and HeLa-Cx43 under control condition (pH 7.4) and after exposure to extracellular pH 7.8 or 8.5. Data are presented as means ± SE, with the number of experiments indicated within each bar. $^{**}P < 0.01$; ns, not significant. Values recorded in 20 cells per experiment were included. *D*: effects of blockers on Etd uptake rates. Experiments were performed in HeLa-Cx43 cells under control condition and after exposure to pH 8.5, followed by treatment with 200 μM La^{3+} or 1 mM probenecid, blockers of connexin and pannexin HCs, respectively. Each value corresponds to means ± SE of 20 cells from 4 independent experiments. $^{***}P < 0.001$.

ments, cells plated onto glass coverslips were washed twice with recording solution and incubated in 5 μM Etd, and fluorescence intensity was recorded in regions of interest of different cells with a water immersion Olympus 51W1I upright microscope. Images were captured with a Q Imaging model Retiga 13001 fast cooled monochromatic digital camera (12-bit; Qimaging, Burnaby, BC, Canada) every 20 s (exposure time = 30 ms; gain = 0.5) and Metafluor software (version 6.2R5; Universal Imaging, Downingtown, PA) was used for image analysis and fluorescence quantification. Slopes were calculated using Microsoft Excel software and expressed as arbitrary units per minute.

Electrophysiology. Cells seeded on glass coverslips were placed onto a custom made chamber mounted on the stage of an inverted Olympus IX-51 microscope. The extracellular bath solution contained (in mM) 140 NaCl, 5.4 KCl, 1 $MgCl_2$, 1.8 $CaCl_2$, 2 $BaCl_2$, and 10 HEPES, pH 7.4. For whole-cell patch-clamp experiments, the pipette solution contained (in mM) 130 CsCl, 10 AspNa, 0.26 $CaCl_2$, 1 $MgCl_2$, 2 EGTA, 7 TEA-Cl, and 5 HEPES, pH 7.2. Whole cell currents were recorded as described previously (60). Patch electrodes were made from borosilicate glass capillaries using a Flaming/Brown micropipette puller (P-87, Sutter Instruments, Union City, CA). The tip resistance was 5–10 MΩ when filled with pipette solution. Currents were filtered at 1 kHz and sampled at 5 kHz. Then, records were filtered with a digital low pass filter of 0.5 kHz. Data acquisition and analysis were performed using pClamp 9 (Axon Instruments, Novato, CA).

Surface protein biotinylation and Western blot analysis. Cell cultures seeded on 100-mm culture dishes were washed three times with recording solution. Then, 3 ml of sulfo-NHS-SS-biotin (0.5 mg/ml) were added to each dish and incubation proceeded for 30 min at 4°C. Cells were then washed three times with recording solution containing 15 mM glycine, pH 8.0, to quench unreacted biotin. Afterward, cells were harvested by scraping with a rubber policeman in the presence of protease and phosphatase inhibitors (as for Western blot analysis, see below) and centrifuged at 4 *g* for 2 min. Pellets were sonicated with a Microson Sonicator ultrasonic homogenizer (Misonix, Farmingdale, NY) on ice in 50 μl lysis buffer containing protease (200 μg/ml soybean trypsin inhibitor, 1 mg/ml benzamidine, 1 mg/ml aminocaproic acid, and 2 mM PMSF) and phosphatase (20 mM $Na_4P_2O_7$ and 100 mM NaF) inhibitors. The immobilized NeutrAvidin (1 μl of

NeutrAvidin per 3 μg of biotinylated protein) was added to each sample, and the mixture was maintained for 1 h at 4°C. Then, 1 ml of binding buffer (recording solution at, pH 7.2, plus 0.1% SDS and 1% NP-40) was added, mixed by soft vortexing, and centrifuged at 4 *g* for 2 min. Then, the supernatant was removed and 40 μl recording solution at pH 2.8 plus 0.1 M glycine were added to the pellet, mixed gently, and centrifuged again at 4 *g* for 2 min. The supernatant was removed, and pH was adjusted to 7.4 immediately by adding 10 μl of 1 M Tris, pH 7.4. Protein levels of cell lysates were measured with the Bio-Rad protein assay (Bio-Rad Laboratories, Richmond, CA). Samples were then analyzed by immunoblotting. Briefly, aliquots of cell lysates (100 μg of protein) were resuspended in 1× Laemmli sample buffer, separated on 8% SDS-PAGE, and electrotransferred to nitrocellulose sheets. Nonspecific protein binding was blocked by incubating the nitrocellulose sheets in 5% nonfat milk prepared in PBS for 60 min, and then blots were incubated with primary polyclonal anti-Cx43, anti-hemagglutinin, or anti-Cx43 NH_2-terminal antibody overnight at 4°C, followed by six 20-min PBS washes. Each primary antibody was diluted in 5% nonfat milk in PBS. Blots were incubated with goat anti-rabbit secondary antibody conjugated to horseradish peroxidase (1:5,000 in 5% nonfat milk in PBS). Antigen-antibody complexes were detected by ECL using the SuperSignal kit according to the manufacturer's instructions. Resulting immunoblot signals were scanned and densitometric analyses were performed using the Scion Image software (Scion, Frederick, MD). Relative levels of surface Cxs were determined by densitometry.

Immunofluorescence experiments. Cells plated onto glass coverslips were fixed with 70% ethanol for 20 min at −20°C and incubated in blocking solution (70% goat serum, 30% PBS, and 1% BSA) for 30 min at room temperature. Then, cells were incubated overnight at 4°C with a rabbit anti-Cx43 polyclonal primary antibody (1:500 in blocking solution) characterized and described previously (6). Preparations were then washed six times with PBS for 5 min, incubated with the GARF-conjugated anti-rabbit IgG antibody for 1 h at 4°C, and submitted again to six 5-min PBS washes at room temperature. Finally, coverslips were mounted using Fluoromont G and examined with an Olympus FW100 confocal microscope equipped with a ×100 1.4 NA lens. Preparations were excited at 488 nm, and emission between 505 and 525 nm was collected.

Ca^{2+} measurements in liposome preparations containing purified Cx43-HCs. Determinations of Ca^{2+} transport were performed on liposomes containing purified Cx43 HCs prepared as described previously (3). Briefly, Cx43 with a COOH-terminal His tag, expressed using a baculovirus/insect-cell expression system, was purified based on its affinity for Ni^{2+}. The purified protein, solubilized in *n*-decyl-β-D-maltopyranoside, was dephosphorylated with alkaline phosphatase immobilized on agarose to assure that HCs were permeable and then reconstituted in L-α-phosphatidylcholine:L-α-phosphatidylserine, 2:1 molar ratio. Unilamellar liposomes and proteoliposomes of <100 nm in diameter were generated by dialysis/extrusion (3), and their size was confirmed by dynamic light scattering measurements (BI 200SM; Brookhaven Instruments, Holtsville, NY). Calcium green-2 was trapped inside the liposomes and proteoliposomes during the extrusion process at a concentration of 40 mM, in 10 mM KCl, 5 mM EDTA, and 10 mM HEPES, pH 7.4. After a 10-fold dilution in the same buffer, but without calcium green-2, the extraliposomal probe was removed by gel filtration. Fluorescence from calcium green-2, which increases upon Ca^{2+} binding (17), was measured on a Hitachi F-7000 spectrofluorimeter (Tokyo, Japan) at excitation and emission wavelengths of 503 and 536 nm, respectively.

Statistical analysis. Data are presented as means ± SE, and *n* represents the number of independent experiments. Means were compared using paired and unpaired *t*-tests for two group variables and one-way ANOVA followed by a Bonferroni posttest in multiple data sets. Differences between proportions were assessed using descriptive statistics. Differences were considered significant at $P < 0.05$. Statistics were performed using Microsoft Excel and the GraphPad Prism 4.0 (2003).

RESULTS

It has previously been shown that HeLa cells transfected with Cx43, but not parental HeLa cells, express functional Cx HCs (12, 14, 60, 71). In agreement with those studies, we detected similar Cx43 reactivity in the cell membrane and intracellular compartments of isolated HeLa-Cx43 cells, using confocal immunofluorescence, while no membrane signal was detected in parental cells (Fig. 1*A*). The presence of Cx43 forming undocked HCs at the HeLa-Cx43 cell membrane was confirmed by surface protein biotinylation and Western blot analyses (see Fig. 6). No evident differences in either cell morphology or Cx43 immunoreactivity pattern were detected in HeLa-Cx43 cells exposed for up to 10 min to pH 8.5, compared with control cells exposed to extracellular pH 7.4 (Fig. 1*A*).

In HeLa-Cx43 and -parental cells under control conditions (pH 7.4 and 1.8 mM Ca^{2+}/1 mM Mg^{2+}), the Etd uptake rate was <0.04 arbitrary units/min (Fig. 1, *B* and *C*). Exposure to extracellular pH 8.5 rapidly increased (<15 s) the rate of Etd uptake (Fig. 1*B*) by <75% in Cx43-transfected HeLa cells (Fig. 1*C*; $P < 0.01$). When HeLa-Cx43 were reexposed to control extracellular pH, the Etd uptake rate returned to baseline levels, whereas reexposure to pH 8.5 increased the Etd uptake rate, similar to the first alkaline exposure, indicating complete reversibility of the response (Fig. 1*B*). In contrast, no change in the Etd uptake rate was observed in HeLa-parental cells subjected to the same experimental protocol (Fig. 1, *B* and *C*; $P > 0.05$), or in HeLa cells transfected with the vector used for Cx43 expression, without insert (not shown), indicating that the above responses were not induced by the transfection protocol. Cells exposed to pH 7.8 showed an Etd uptake rate with a clear tendency above the control cells at pH 7.4 or parental cells exposed to pH 8.5 (Fig. 1*C*). Notably, the increase in the Etd uptake rate induced by pH 8.5 in HeLa-Cx43 cells was abolished by 200 μM La^{3+}, a Cx HC blocker (48), but remained unaffected by the application of 1 mM probenecid, a Px1 HC inhibitor (59) (Fig. 1*D*).

To further characterize the pathway through which exposure to extracellular pH 8.5 increases the membrane permeability of HeLa-Cx43 cells, we used the whole cell voltage-clamp technique to study macroscopic and microscopic currents. As previously shown (60), at V = 0 mV the current value was zero (Fig. 2*A*), characteristic of a nonselective membrane channel such as Cx and Px HCs (2, 12). Exposure to pH 8.5 increased the total current ~1.5 times (Fig. 2, *A* and *B*). Moreover, rectangular voltage pulses from 0 mV to +80 mV (5-s duration) evoked current transitions that were more numerous and presented a much shorter "on time" (latency; 0.8 ± 0.4 s and 2.2 ± 0.5 s, respectively) at pH 8.5 than at pH 7.4 (Fig. 2*C*). When the membrane potential was brought to −20 mV, a tail current was readily apparent, with unitary events with longer "off time" in cells exposed to pH 8.5, compared with control cells (7.5 ± 1.2 s and 0.9 ± 0.6 s, respectively; Fig. 2*D*, compare pH 7.4 and 8.5). Both, the current evoked by voltage pulses from 0 to +80 mV and the tail unitary currents generated by voltage pulse from +80 to −20 mV were abolished by 200 μM La^{3+} (Fig. 2, *C* and *D*, *bottom traces*, respectively), a blocker of Cx HCs that does not affect Px HCs (48). The tail

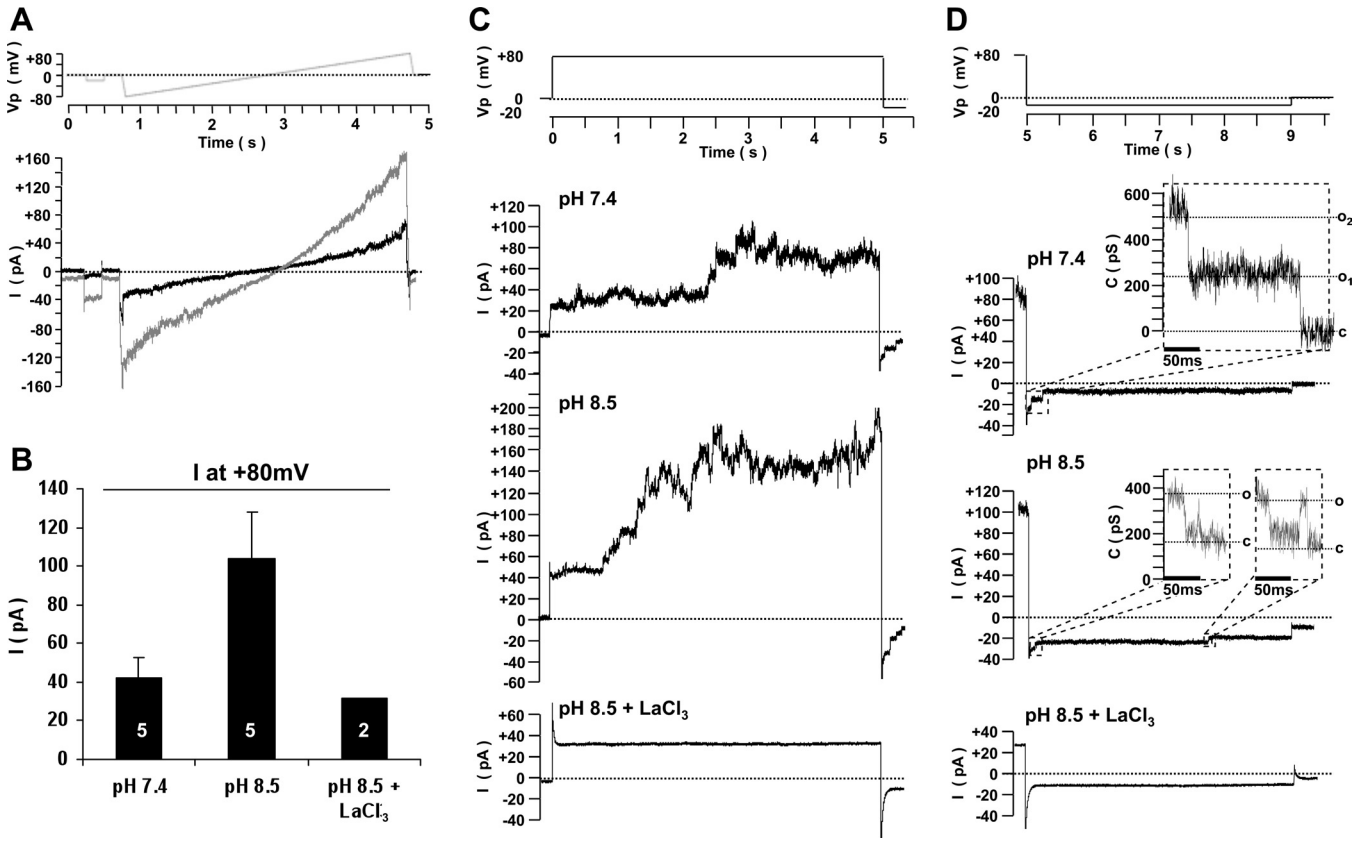

Fig. 2. Extracellular pH 8.5 increases the Cx43EGFP HC-mediated currents. *A*: representative voltage-clamp recordings showing the macroscopic currents recorded in HeLaCx43EGFP cells exposed first to extracellular pH 7.4 (black) and then to pH 8.5 (gray) using a voltage-ramp protocol. *B*: summary of macroscopic currents recorded at +80 mV. Each bar represents means ± SE, with the number of cells indicated within each bar. *C*: macroscopic current recorded in HeLaCx43EGFP cells subjected first to extracellular pH 7.4, followed by exposure to pH 8.5, as a function of a rectangular voltage protocol from zero to +80 mV. Note the increase of the current at pH 8.5, which upon treatment with La^{3+} (100 μM, $LaCl_3$) was completely abrogated. *D*: current recorded at −20 mV, after the application of a rectangular voltage protocol of +80 mV during 5 s. Values of discrete current transitions were converted point-by-point to conductance values indicated in *insets*. The gγ values of transitions recorded under pH 7.4 and pH 8.5 varied from 220 to 250 pS. The open (o) and closed (c) HC states are indicated. *I-V*, current-voltage relationship.

current generated with a step from +80 mV to −20 mV presented unitary events with similar single-channel conductances of ~220 pS at pHs 7.4 and 8.5 (Fig. 2*D*, *insets*), indicative of Cx43 HCs (12), and different from Px1 HCs (475–550 pS) (2). The combined data strongly suggest that Cx43 HCs are the pathway for the increased Etd uptake upon alkalinization.

Since extracellular alkalinization induces cell death associated with increased intracellular [Ca^{2+}] (39), variations in intracellular Ca^{2+} levels upon Cx43 HC activation by extracellular pH 8.5 were monitored in cells preloaded with the Ca^{2+} indicator fluo 4. Extracellular alkalinization increased the peak fluo 4 fluorescence in HeLa-Cx43 cells but did not affect it in parental cells (Fig. 3*A*; $P < 0.01$). The increase in Ca^{2+}-dependent fluorescence observed in HeLa-Cx43 cells was rapid (<15 s), reaching a steady-state after <2 min (Fig. 3*B*). As expected for influx through activated Cx43 HCs, raising the transmembrane Ca^{2+} gradient by increasing extracellular [Ca^{2+}] to 10 mM promoted an additional increase in the alkalinization-triggered fluo 4 fluorescence in HeLa-Cx43 cells, reaching a new steady-state value after ~45 s (Fig. 3, *A* and *B*; $P < 0.01$). The rate of increase in fluo 4 emission upon extracellular alkalinization was ~2.3-fold higher in 10 vs. 1.8 mM extracellular [Ca^{2+}] (Fig. 3, *B* and *C*; $P < 0.001$). Reexposure of HeLa-Cx43 cells to the control solution (pH 7.4, 1.8 mM Ca^{2+}/1 mM Mg^{2+}) lowered the fluo 4 signal to levels that approached control values (Fig. 3*B*). In contrast to the results in HeLa-Cx43, exposure of HeLa-parental cells to pH 8.5, either in the presence of 1.8 or 10 mM extracellular [Ca^{2+}], had little effect on both fluo 4 fluorescence emission and its rate of increase (Fig. 3, *A* and *C*; $P > 0.05$). Interestingly, despite the reduction in the open probability induced by extracellular Ca^{2+} at physiological extracellular pH (12), the membrane permeability to Etd in cells exposed to pH 8.5 in the presence of 10 mM Ca^{2+} was still higher than that in control cells and was completely inhibited by 200 μM La^{3+} (Supplemental Fig. 1; Supplemental Material for this article is available online at the *Am J Physiol-Cell Physiol* website). In agreement with the low open probability of Cx43 HCs in cells exposed to physiological [Ca^{2+}] at pH 7.4, increasing extracellular [Ca^{2+}] to 10 mM did not reduce Etd uptake (compare Fig. 1*C* and Supplemental Fig. 1). Notably, the increase in Etd uptake recorded at pH 8.5 in the presence of 1.8 mM and 10 mM extracellular Ca^{2+} was similar, indicating that the increase in Etd uptake induced by extracellular alkalinization is insensitive to Ca^{2+}.

To further evaluate the Cx43 dependence in the responses described above, intracellular Ca^{2+} levels were measured us-

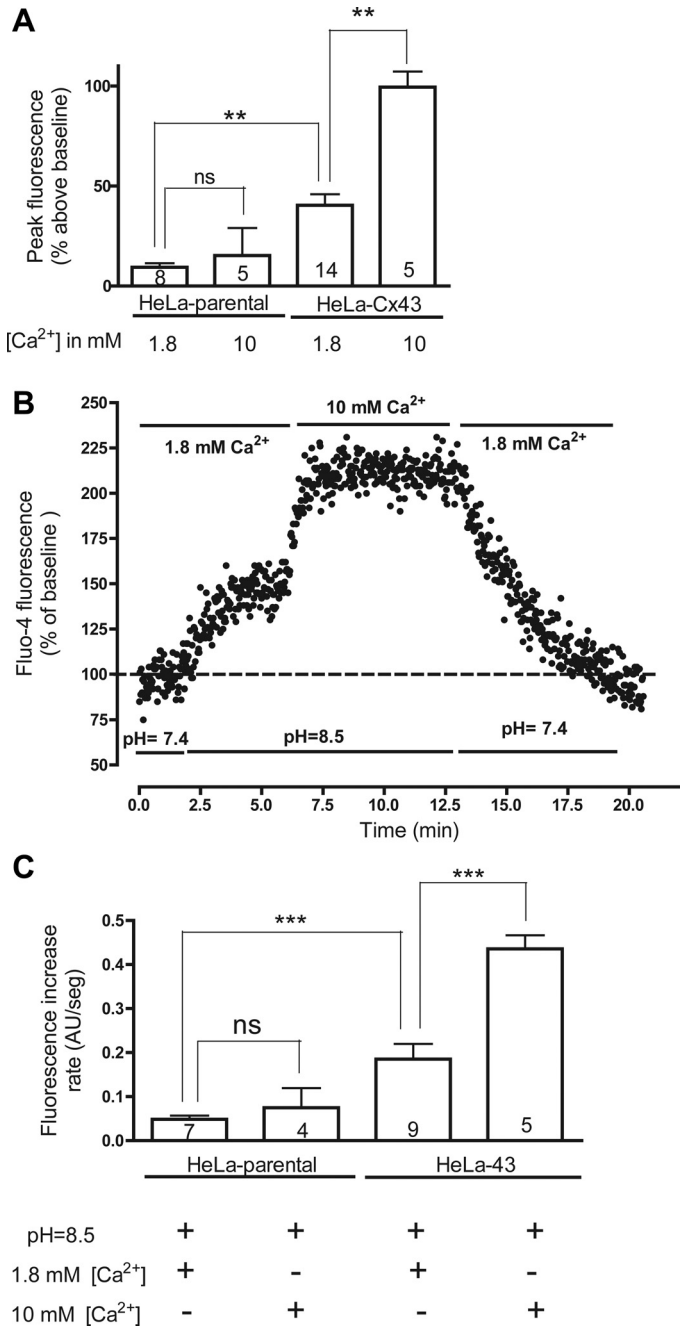

Fig. 3. Extracellular alkalinization increases the intracellular Ca^{2+} levels of HeLa-Cx43 cells in an extracellular Ca^{2+} concentration ([Ca^{2+}])-dependent way. *A*: peak fluo 4 fluorescence increase in HeLa-parental and HeLa-Cx43 after changing the extracellular pH from 7.4 to 8.5 in the presence of 1.8 or 10 mM Ca^{2+}. Values are percentage above the baseline levels, and data are means ± SE (number of experiment, *n*, indicated inside each bar). Each independent experiment was the average of including at least 8 cells. *B*: representative time-lapse recordings of the relative fluo 4 fluorescence intensity of HeLa-Cx43 cells exposed to saline solutions containing different [Ca^{2+}] and pH. Dotted line indicates the mean relative fluorescence intensity under the control conditions (pH 7.4; 1.8 mM Ca^{2+} and 1 mM Mg^{2+}). *C*: average fluo 4 fluorescence increase rate of HeLa-parental and HeLa-Cx43 cells exposed to pH 8.5 in the presence of 1.8 or 10 mM extracellular Ca^{2+}. $^{**}P < 0.01$; $^{***}P < 0.001$.

ing fura red in cocultures of HeLa-parental and HeLa-Cx43EGFP cells; the latter have been shown to produce functional HCs (12, 60). Different to most Ca^{2+} indicators, fluorescence of fura red decreases upon Ca^{2+} binding. As shown in Fig. 4*A*, extracellular alkalinization in the presence of 1.8 mM extracellular [Ca^{2+}] induced a larger increase in intracellular Ca^{2+} levels in Cx43EGFP-expressing cells [Cx43EGFP (+)] than in HeLa-parental cells [Cx43EGFP (−)]. Moreover, the alkaline-induced response was much higher after the extracel-

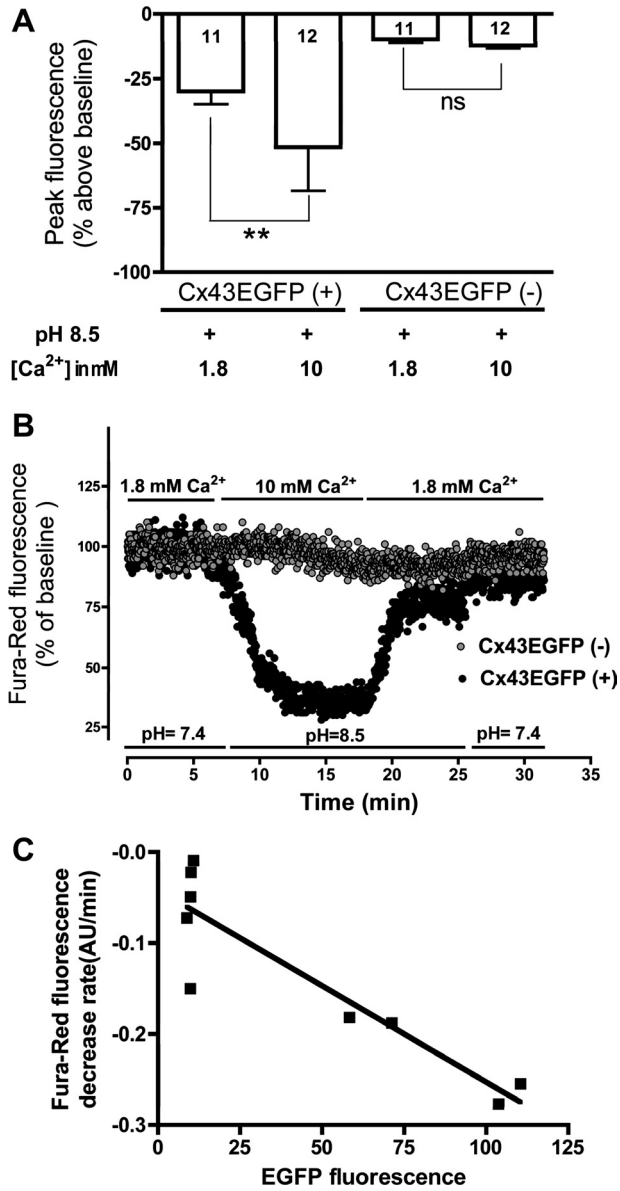

Fig. 4. Increase in the intracellular Ca^{2+} levels induced by extracellular alkalinization is related to the Cx43EGFP levels. *A*: peak fura red fluorescence intensity in HeLa-parental [Cx43EGFP (−)] and HeLa-Cx43EGFP [Cx43EGFP (+)] cells after exposure to pH 8.5 in the presence of 1.8 or 10 mM extracellular [Ca^{2+}]. Values are expressed as percentage of change respect to baseline. $^{**}P < 0.01$. *B*: representative time-lapse recording of the relative fura red fluorescence intensity of cocultured [Cx43EGFP (−)] and [Cx43EGFP (+)] cells exposed to solutions containing different [Ca^{2+}] and pH. Values are percentage with respect to baseline levels at pH 7.4 and 1.8 mM extracellular Ca^{2+} and 1 mM Mg^{2+}. *C*: inverse correlation between Cx43EGFP fluorescence intensity and fura red fluorescence rate of change right after exposure to pH 8.5. Line indicates the linear regression curve ($r^2 = -0.84$; $P < 0.001$; $n = 10$ cells).

lular [Ca^{2+}] was raised to 10 mM only in Cx43EGFP-expressing cells (Fig. 4*A*; $P < 0.01$). In the latter, exposure to 10 mM extracellular Ca^{2+} at pH 8.5 rapidly decreased the fura red signal (<15 s), reaching a lower steady-state value <60% below the baseline (Fig. 4*B*, black circles). At extracellular pH 8.5, reduction of extracellular [Ca^{2+}] to 1.8 mM decreased the fura red signal, reaching a new steady state <30% below baseline, revealing again the extracellular Ca^{2+} dependence of the observed fura red fluorescence responses. Only a small reduction in fura red fluorescence (<10%) occurred in parental cells during the recorded time period (Fig. 4, *A* and *B*, white circles). The decrease in fura red fluorescence rate elicited by extracellular alkalinization in the presence of 1.8 mM Ca^{2+} was inversely related to the Cx43EGFP fluorescence intensity (Fig. 4*C*; $r^2 = 0.84$; $P < 0.001$; $n = 10$). A similar relationship was found in cells exposed to pH 8.5 in the presence of 10 mM extracellular [Ca^{2+}] ($r^2 = 0.94$; $P < 0.001$; $n = 10$; data not shown).

Since the increase in membrane permeability to Etd could result from a rapid rise in the number of HCs in the cell membrane, we tested if exposure to extracellular alkalinization affects the amount of Cx43EGFP at the cell membrane. To this end, we measured the fluorescence intensity of different membrane domains using confocal microscopy and found that exposure to pH 8.5 did not affect the fluorescence over a time course comparable to that of the Etd uptake and intracellular Ca^{2+} measurements described above (Fig. 5). Moreover, we found that 12-min exposure to a saline solution containing 10 mM Ca^{2+} did not affect the Cx43EGFP fluorescence present in the cell membrane (Fig. 5*C*).

The COOH-terminal domain of Cx43 has been involved in the sensitivity to intracellular pH and "chemical" gating of Cx43-based gap junction channels and HCs (16). To test its potential role in the effect of extracellular alkalinization, we studied HeLa cells expressing a truncated Cx43 (Cx43Δ257), lacking most of the C-terminal domain. These cells have been shown to form HCs that are activated by exposure to Ca^{2+}/Mg^{2+}-free solutions (60). To further confirm the previous findings, surface membrane proteins of HeLa-Cx43Δ257 and HeLa-Cx43 cells were biotinylated and levels of Cxs were evaluated by Western blot analysis of pulled down proteins, using an antibody directed against an NH_2-terminal epitope. Blots revealed the presence of both proteins at the cell surface, at comparable levels (Fig. 6*A*; $P > 0.05$). However, in HeLa-Cx43Δ257 cells, the rate of fluo 4 signal increase was ~1.8-fold that of HeLa-Cx43 cells (Fig. 6*B*; $P < 0.05$). We have previously shown that the HC-mediated membrane permeability to Etd of Cx43 and Cx43Δ257 transfectants under resting conditions is similar (60). In summary, as opposed to the gating of Cx43 intercellular channels by intracellular pH (16), the effect of extracellular alkalinization on Cx43 HCs is not abolished by the COOH-terminal domain truncation.

As shown above, sustained activation of Cx43 HCs by exposure to pH 8.5 elicited a higher steady-state intracellular Ca^{2+} level (Fig. 3*B*) but induced a continuous increase in Etd uptake rate (Fig. 1*B*). The differences in kinetics could be explained by a change in the HC selectivity or by the presence of mechanism(s) with capacity to control the raise in intracellular [Ca^{2+}]. In support of the latter possibility, we found that treatment with 1 mM (Fig. 7*A*) or 5 mM (not shown) sodium orthovanadate, which blocks PMCA pumps (13), results in a higher plateau in the fluo 4 fluorescence induced by pH 8.5 in cells expressing Cx43 HCs (Fig. 7*A*; $P < 0.05$). Exposure to pH 8.5 in the presence of sodium orthovanadate also caused a larger reduction in fura red fluorescence of HeLa-Cx43EGFP cells [Fig. 7*B*, Cx43EGFP (+)], not observed in HeLa-parental cells [Fig. 7*B*, Cx43EGFP (−)]. These results suggest that the level of the increase in [Ca^{2+}] induced by extracellular alka-

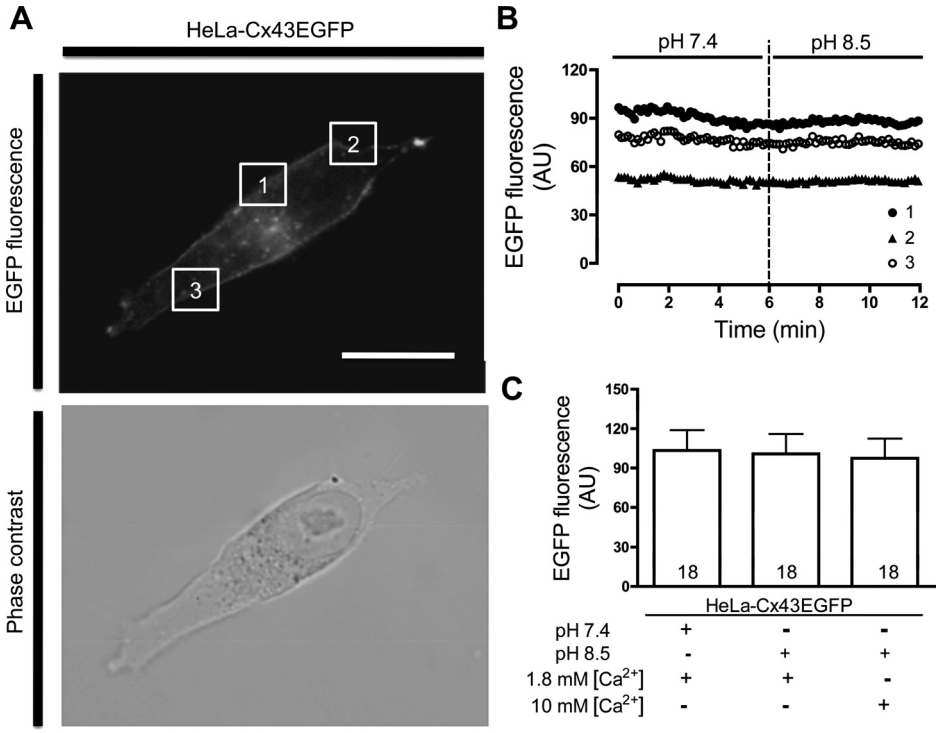

Fig. 5. The plasma membrane HC level is not affected by extracellular alkalinization or high extracellular [Ca^{2+}] in HeLa-Cx43EGFP. *A*: representative confocal image of a HeLa-Cx43EGFP cell showing surface Cx43EGFP signal. Fluorescence at 530 nm (*top*) and corresponding phase contrast image (*bottom*). *B*: continuous EGFP fluorescence intensity recordings from 3 different cell membrane spots of the HeLa-Cx43EGFP cell shown in *A*, before and after exposure to pH 8.5. *C*: average Cx43EGFP fluorescence intensity of membrane domains of HeLa-Cx43EGFP cells in the control conditions, and after exposure to pH 8.5, in the presence of 1.8 or 10 mM extracellular Ca^{2+}. Bars are means ± SE from 18 cells in 6 independent experiments.

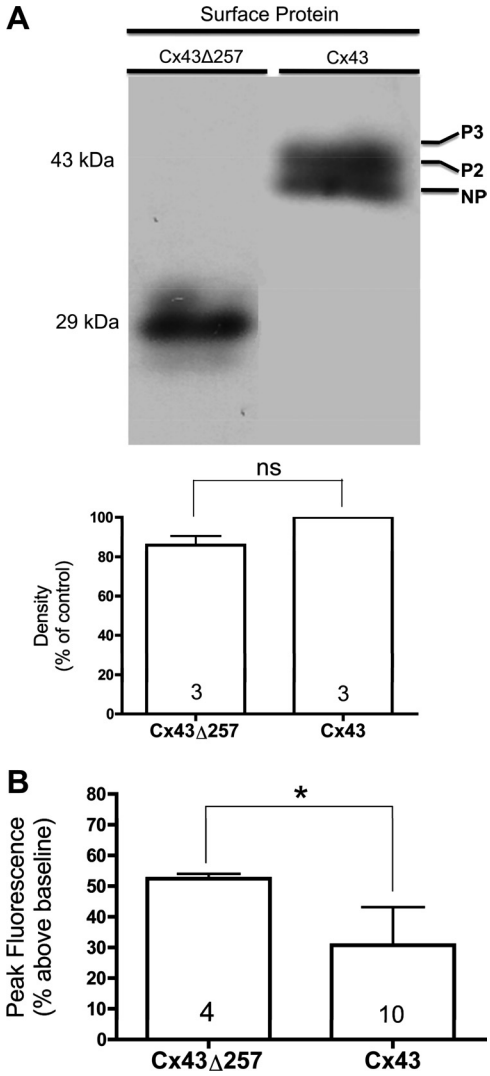

Fig. 6. Increase in intracellular Ca^{2+} levels induced by extracellular alkalinization is not abolished by truncation of the COOH-terminal domain. *A*: HeLa cells transfected with Cx43Δ257 or wild-type Cx43 express comparable levels of surface HCs. HeLa cells transfected with Cx43Δ257 or Cx43 were cultured to similar cell density and surface levels of the corresponding Cx were measured through biotinylation of surface proteins and Western blot analysis using an antibody that recognizes an epitope in the NH_2-terminal region. Equal amounts of total surface protein were loaded in each lane. *Top*: representative Western blot analysis of surface proteins. *Bottom*: Cx43Δ257 levels are expressed as percentage of surface Cx43 levels. *B*: fluo 4 fluorescence increase rate in HeLa-Cx43Δ257 and HeLa-Cx43 after exposure to pH 8.5 for 1 min in the presence of 1.8 mM extracellular [Ca^{2+}]. *$P < 0.05$.

linization is limited by mechanisms that include the PMCA pumps.

Previous studies (29) have shown that Cx43 affects the expression of several proteins, including plasma membrane channels and transporters. Therefore, we decided to confirm the Ca^{2+} permeability of Cx43 HCs more directly. To this end, we performed experiments with purified Cx43 HCs, dephosphorylated and reconstituted in liposomes. Liposomes with or without Cx43 HCs, with the Ca^{2+}-sensitive probe calcium green-2 trapped inside, were prepared as described previously (3). A ~1.8-fold larger increase in the calcium green-2 fluorescence emission occurred upon increasing extraliposomal

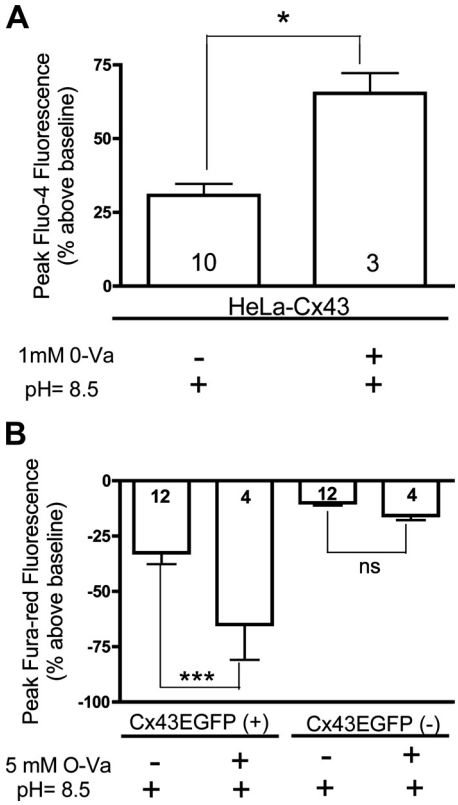

Fig. 7. Increase in intracellular Ca^{2+} levels induced by extracellular alkalinization is more prominent after inhibition of PMCA pumps. *A*: peak fluo 4 fluorescence signal change in HeLa-Cx43 without or with treatment with sodium orthovanadate (O-Va, 1 mM) for 30 min. Cells were exposed to pH 8.5 in the presence of 1.8 mM extracellular [Ca^{2+}]. *B*: peak fura red fluorescence intensity of HeLa-parental [Cx43EGFP (−)] and HeLa-Cx43EGFP [Cx43EGFP (+)] cells without or with treatment with 5 mM O-Va and exposed to pH 8.5 in the presence of 1.8 mM extracellular [Ca^{2+}]. *$P < 0.05$; ***$P < 0.001$.

[Ca^{2+}] from 5 to 20 μM in the presence of dephosphorylated Cx43 HCs (Fig. 8; $P < 0.02$). The increases in fluorescence emission in liposomes lacking Cx43 HCs are due to extraliposomal calcium green-2 not removed by gel filtration (see MATERIALS AND METHODS). These results show that HCs formed by dephosphorylated Cx43 are permeable to Ca^{2+}.

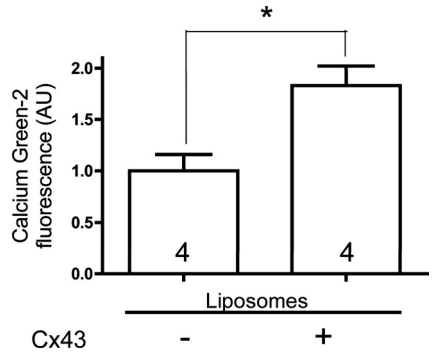

Fig. 8. Purified Cx43 HCs dephosphorylated and reconstituted in liposomes are permeable to Ca^{2+}. Influx of Ca^{2+} into liposomes containing purified Cx43 HCs. Bars show means ± SE, with the number of experiments inside the bars, of the increases in calcium green-2 fluorescence emission (AU). Probe was trapped into liposomes without (−) or with purified Cx43. *$P < 0.02$, compared with the liposomes without Cx43 HCs.

DISCUSSION

In the present work, we show that Cx43 HCs are rapidly and reversibly activated by extracellular alkalinization to pH 8.5, despite the presence of high extracellular [Ca^{2+}], which blocks HCs. Activation of Cx43 HCs was directly related to increased Ca^{2+} influx, leading to a higher steady-state intracellular Ca^{2+} level, limited in magnitude by the activity of PMCA pumps, as expected from the increase in intracellular Ca^{2+} signal. Purified Cx43 HCs, dephosphorylated and reconstituted in liposomes, allow passage of Ca^{2+}, providing direct evidence for Ca^{2+} permeation through activated HCs. In addition, we show that the COOH-terminal domain of Cx43 is not involved in sensing or mediating the HC response to extracellular alkalinization and that it might even have a negative regulatory effect. This contrasts with the inhibitory effect of intracellular acidification, which depends on the presence of the COOH-terminal domain. Our data strongly suggest that Cx43 HCs activated by extracellular alkalinization are permeable to Ca^{2+} and that they are likely to play a relevant role controlling intracellular Ca^{2+} homeostasis under physiological and pathological conditions in which extracellular alkalinization occurs.

Cx43 HC activation by extracellular pH 8.5. In addition to Cxs, pannexins (Pxs) can form functional HCs in vertebrate cells (64). Cx and Px HCs are permeable to ions and small molecules and are often endogenously coexpressed in diverse cell types (64). The use of heterologous expression systems and pharmacological approaches has been valuable to discriminate between the relative contributions of Cx and Px HCs (48, 59, 61). On the one hand, although HeLa cells have detectable Px1 levels (60), neither surface Px1 expression nor Px1 HC activity has been detected (28, 60), i.e., functional Px1 HCs are not expressed in these cells. Moreover, we found that extracellular pH 8.5 does not induce Px1 HC activation at the cell membrane since probenecid, a Px1 HC blocker (48), did not prevent the alkalinization-induced HC activation. On the other hand, HeLa cells transfected with Cx43, but not parental HeLa cells, express functional Cx HCs (14, 60, 71). In support of the latter, we found that increased Etd uptake induced by pH 8.5 was abolished by La^{3+}, a known inhibitor of Cx HCs (59). These observations support the notion that HeLa cells do not express functional HCs formed by Pxs or endogenous Cxs. In agreement with the above observations, electrophysiological measurements revealed the presence of nonselective membrane channels (zero current at V = 0 mV) and only discrete single channels events of ~220 pS in cells expressing Cx43EGFP HCs as described previously (12).

Exposure to extracellular solution with pH 8.5 rapidly increased the Cx HC-dependent Etd uptake rate, revealing activation of Cx43 HCs. This was not due to an increase in HC levels at the cell membrane because we did not detect changes cellular distribution of wild-type Cx43 (using immunofluorescence and confocal detection) or changes in surface level of Cx43EGFP (using confocal detection) in response to pH 8.5. Therefore, it is likely that alkaline pH activates a gating mechanism leading to opening of Cx43 HC. In agreement with this interpretation, activation of current events at pH 8.5 occurred with much less delay and the "off time" of single channels was much longer than at pH 7.4, which are indications of an increase in open probability. Therefore, the increase in HC activity was due to an increase in open probability and not to increased levels of HCs at the cell membrane, as observed in cells under metabolic inhibition or FGF-1 treatment (52, 58, 60). Similar to our observations on Cx43 HCs, Cx26 and Cx46 HCs expressed in *Xenopus* oocytes are rapidly activated by extracellular alkalinization (55, 69), and for Cx26 HCs, atomic force microscopy data suggest an increase in the external HC-pore diameter (76).

Intracellular acidification reduces the activity of intercellular gap-junction channels formed by diverse Cxs (27, 49), and intracellular alkalinization increases the open probability of gap junction channels formed by Cx45 (46) or Cx57 (45). One putative domain involved in sensing the intracellular pH changes is the cytoplasmic COOH-terminal domain, which, at least in Cx43-based intercellular channels, has been proposed to act as part of a gating "ball-and-chain" mechanism (16). Our findings show that the COOH-terminal domain of Cx43 is not required for the alkalinization-induced HC activation. We found that at comparable plasma membrane protein levels, the increase in Etd uptake was more pronounced in cells expressing Cx43Δ257 compared with those expressing wild-type Cx43. These data suggest that truncated HCs are released from the inhibition mediated by the COOH-terminal domain, expected from a "ball-and-chain" mechanism activated by acid pH, which possibly interferes with or reduces HC activation induced by pH 8.5. Our results clearly show that the Cx43 HC response to extracellular alkalinization cannot be explained by a "ball-and-chain" mechanism that involves the COOH-terminal domain. The findings suggest involvement of other protein domain(s). Further mutagenesis studies will be needed to identify the domains involved in the gating of Cx43 HCs by extracellular alkalinization.

Cx43 HCs permeability to Ca^{2+}. The close relationship between Cx43EGFP levels and fura red fluorescence intensity changes upon exposure to pH 8.5 indicates that cells expressing more HCs also display more Ca^{2+} influx. In contrast, no significant increase in intracellular Ca^{2+} levels was elicited by extracellular alkalinization in parental cells lacking functional HCs (HeLa-parental cells or mock-transfected HeLa cells). These findings, together with the higher Cx43 HC activity revealed by Etd uptake measurements, suggest that Cx43 HCs allow Ca^{2+} influx.

The rise in intracellular [Ca^{2+}] upon activation of HCs by extracellular alkalinization is compatible with the notion of passive Ca^{2+} influx through HCs; the elevation in intracellular Ca^{2+} signal was enhanced by increases in the Ca^{2+} electrochemical driving force. In support of Ca^{2+} influx through HCs, an increase in intracellular [Ca^{2+}] was reported in thapsigargin-treated HeLa cells expressing Cx43 upon switching from a Ca^{2+}-free to a saline solution containing 1.3 mM [Ca^{2+}] (71). In that study, the rise in intracellular [Ca^{2+}] was inhibited by Gap26, a Cx mimetic peptide known to inhibit Cx43 HCs, suggesting Cx43 HCs as a pathway for Ca^{2+} influx (71). In the present work, we demonstrated that purified and dephosphorylated Cx43, known to form functional HCs in liposomes (3), increased intraliposomal Ca^{2+} upon increasing extra-liposomal [Ca^{2+}], indicating that Cx43 HCs provide a transmembrane Ca^{2+} pathway. Quantitative correlation between the data in cells and proteoliposomes is difficult because the HC responses are likely affected by posttranslational modifications and/or the modulatory effect of intracellular binding partners found in

vivo. Nevertheless, all of our data support the notion of Ca^{2+}-permeable Cx43 HCs.

Increase in Cx43 HC activity has been demonstrated previously in the presence of physiological extracellular concentration of divalent cations. Examples include astrocytes (11), cardiomyocytes (30) and kidney epithelial cells (70) under metabolic inhibition, cortical astrocytes subjected to hypoxia-reoxygenation (44), and cells treated with proliferative or proinflammatory agents (14, 54, 60). Here, we found that activation of Cx43 HCs induced by extracellular alkalinization occurs even in the presence of 10 mM extracellular [Ca^{2+}], showing that Cx43 HC gating by alkaline pH overcomes the reduction in open probability induced by extracellular divalent cations. Alternatively, a conformational change induced by pH 8.5 could affect the open probability through reduction in the HC extracellular Ca^{2+} sensitivity.

Since Cx43 is ubiquitously expressed (62), it is possible that Cx43 HCs serve as a membrane pathway for Ca^{2+} influx in a variety of cell types, mediating diverse Ca^{2+}-dependent physiological and pathological responses. Accordingly, it was recently reported that FGF-1 increases the intracellular [Ca^{2+}] in Cx43-transfected HeLa cells but not in parental cells (60). The tissues in which opening of Cx43 HCs by extracellular alkalinization could play relevant roles are the biliary and intestinal epithelium, where Cx43 is expressed (5, 25) and cells are exposed to pH values close to or above 8.0 (21, 35). Ca^{2+} influx via Cx43 HCs might also explain the alkalinization-induced increase in intracellular [Ca^{2+}] through Ca^{2+} influx in vascular endothelial and vascular smooth muscle cells (1, 42, 73). Moreover, Ca^{2+} influx through Cx43 HCs could participate in a range of undesired effects of the hypocalcemia that results from alkalemia. This hypocalcemia has been historically attributed to an increase in binding of Ca^{2+} to proteins such as albumin (40). However, increased Ca^{2+} influx through Cx43 HCs may also play a role. Finally, persistent Ca^{2+} influx via Cx43 HCs might be related to alkalosis-induced cell death, a well-established phenomenon (39). Further work will be needed to define the range of circumstances in which this putative Ca^{2+} influx pathway contributes to intracellular signaling and homeostasis.

ACKNOWLEDGMENTS

The data of this work were presented by Dr. Kurt Schalper as partial fulfillment of the requirements to obtain the degree of Ph.D. in Medical Sciences at the Pontificia Universidad Católica de Chile.

GRANTS

This work was partially supported by Fondo Nacional de Desarrollo Científico y Tecnológico Grants 1070591 (to J. C. Sáez), Núcleo Milenio P04/030-F (to J. C. Sáez), Anillo ACT 71 (to J. C. Sáez), FONDEF D07I1086 (to J. C. Sáez and K. A. Schalper), Texas Advanced Research Program 010674-0046-2007 (to G. A. Altenberg), NIH R01 GM-79629 (to G. A. Altenberg), and NIH R01GM-079629-03S1 (to G. A. Altenberg). K. A. Schalper received a Comisión Nacional de Investigación Científica y Tecnológica and Pontificia Universidad Católica fellowship for graduate studies.

DISCLOSURES

No conflicts of interest, financial or otherwise, are declared by the author(s).

REFERENCES

1. **Austin C, Wray S.** A quantitative study of the relation between intracellular pH and force in rat mesenteric vascular smooth muscle. *Pflügers Arch* 427: 270–276, 1994.
2. **Bao L, Locovei S, Dahl G.** Pannexin membrane channels are mechanosensitive conduits for ATP. *FEBS Lett* 572: 65–68, 2004.
3. **Bao X, Lee SC, Reuss L, Altenberg GA.** Change in permeant size selectivity by phosphorylation of connexin 43 gap-junctional hemichannels by PKC. *Proc Natl Acad Sci USA* 104: 4919–4924, 2007.
4. **Bennett MV, Contreras JE, Bukauskas FF, Sáez JC.** New roles for astrocytes: gap junction hemichannels have something to communicate. *Trends Neurosci* 26: 610–617, 2003.
5. **Bode HP, Wang L, Cassio D, Leite MF, St-Pierre MV, Hirata K, Okazaki K, Sears ML, Meda P, Nathanson MH, Dufour JF.** Expression and regulation of gap junctions in rat cholangiocytes. *Hepatology* 36: 631–40, 2002.
6. **Brañes MC, Contreras JE, Sáez JC.** Activation of human polymorphonuclear cells induces formation of functional gap junctions and expression of connexins. *Med Sci Monit* 8: 313–323, 2002.
7. **Bruzzone S, Guida L, Zocchi E, Franco L, De Flora A.** Connexin 43 hemi channels mediate Ca^{2+}-regulated transmembrane NAD^+ fluxes in intact cells. *FASEB J* 15: 10–12, 2001.
8. **Bukauskas FF, Jordan K, Bukauskiene A, Bennett MV, Lampe PD, Laird DW, Verselis VK.** Clustering of connexin 43-enhanced green fluorescent protein gap junction channels and functional coupling in living cells. *Proc Natl Acad Sci USA* 97: 2556–2561, 2000.
9. **Castro J, Ruminot I, Porras OH, Flores CM, Hermosilla T, Verdugo E, Venegas F, Härtel S, Michea L, Barros LF.** ATP steal between cation pumps: a mechanism linking Na^+ influx to the onset of necrotic Ca^{2+} overload. *Cell Death Differ* 13: 1675–1685, 2006.
10. **Cherian PP, Siller-Jackson AJ, Gu S, Wang X, Bonewald LF, Sprague E, Jiang JX.** Mechanical strain opens connexin 43 hemichannels in osteocytes: a novel mechanism for the release of prostaglandin. *Mol Biol Cell* 16: 3100–3106, 2005.
11. **Contreras JE, Sánchez HA, Eugenín EA, Speidel D, Theis M, Willecke K, Bukauskas FF, Bennett MV, Sáez JC.** Metabolic inhibition induces opening of unapposed connexin 43 gap junction hemichannels and reduces gap junctional communication in cortical astrocytes in culture. *Proc Natl Acad Sci USA* 99: 495–500, 2002.
12. **Contreras JE, Sáez JC, Bukauskas FF, Bennett MV.** Gating and regulation of connexin 43 (Cx43) hemichannels. *Proc Natl Acad Sci USA* 100: 11388–11393, 2003.
13. **De Luisi A, Hofer AM.** Evidence that Ca^{2+} cycling by the plasma membrane Ca^{2+}-ATPase increases the 'excitability' of the extracellular Ca^{2+}-sensing receptor. *J Cell Sci* 116: 1527–1538, 2003.
14. **De Vuyst E, Decrock E, De Bock M, Yamasaki H, Naus CC, Evans WH, Leybaert L.** Connexin hemichannels and gap junction channels are differentially influenced by lipopolysaccharide and basic fibroblast growth factor. *Mol Biol Cell* 18: 34–46, 2007.
15. **De Vuyst E, Wang N, Decrock E, De Bock M, Vinken M, Van Moorhem M, Lai C, Culot M, Rogiers V, Cecchelli R, Naus CC, Evans WH, Leybaert L.** Ca^{2+} regulation of connexin 43 hemichannels in C6 glioma and glial cells. *Cell Calcium* 46: 176–187, 2009.
16. **Delmar M, Coombs W, Sorgen P, Duffy HS, Taffet SM.** Structural bases for the chemical regulation of connexin43 channels. *Cardiovasc Res* 62: 268–275, 2004.
17. **Eberhard M, Erne P.** Calcium binding to fluorescent calcium indicators: calcium green, calcium orange and calcium crimson. *Biochem Biophys Res Commun* 180: 09–215, 1991.
18. **Ebihara L.** New roles for connexons. *News Physiol Sci* 18: 100–103, 2003.
19. **Eisner DA, Kashimura T, Venetucci LA, Trafford AW.** From the ryanodine receptor to cardiac arrhythmias. *Circ J* 73: 1561–1567, 2009.
20. **Elfgang C, Eckert R, Lichtenberg-Frate H, Butterweck A, Traub O, Klein RA, Hulser DF, Willecke K.** Specific permeability and selective formation of gap junction channels in connexin-transfected HeLa cells. *J Cell Biol* 129: 805–817, 1995.
21. **Evans DF, Pye G, Bramley R, Clark AG, Dyson TJ, Hardcastle JD.** Measurement of gastrointestinal pH profiles in normal ambulant human subjects. *Gut* 29: 1035–1041, 1988.
22. **Evans WH, De Vuyst E, Leybaert L.** The gap junction cellular internet: connexin hemichannels enter the signalling limelight. *Biochem J* 397: 1–14, 2006.
23. **Faigle M, Seessle J, Zug S, El Kasmi KC, Eltzschig HK.** ATP release from vascular endothelia occurs across Cx43 hemichannels and is attenuated during hypoxia. *PLoS One* 3: 2801, 2008.
24. **Franco L, Zocchi E, Usai C, Guida L, Bruzzone S, Costa A, De Flora A.** Paracrine roles of NAD^+ and cyclic ADP-ribose in increasing intra-

cellular calcium and enhancing cell proliferation of 3T3 fibroblasts. *J Biol Chem* 276: 21642–21648, 2001.
25. **Guttman JA, Lin AE, Li Y, Bechberger J, Naus CC, Vogl AW, Finlay BB.** Gap junction hemichannels contribute to the generation of diarrhea during infectious enteric disease. *Gut* 59: 218–226, 2009.
26. **Hawat G, Benderdour M, Rousseau G, Baroudi G.** Connexin 43 mimetic peptide Gap26 confers protection to intac heart against myocardial ischemia injury. *Pflügers Arch* 460: 583–592, 2010.
27. **Harris AL.** Emerging issues of connexin channels: biophysics fills the gap. *Q Rev Biophys* 34: 325–472, 2001.
28. **Huang Y, Grinspan JB, Abrams CK, Scherer SS.** Pannexin1 is expressed by neurons and glia but does not form functional gap junctions. *Glia* 55: 46–56, 2007.
29. **Iacobas DA, Iacobas S, Spray DC.** Connexin-dependent transcellular transcriptomic networks in mouse brain. *Prog Biophys Mol Biol* 94: 169–185, 2007.
30. **John SA, Kondo R, Wang SY, Goldhaber JI, Weiss JN.** Connexin-43 hemichannels opened by metabolic inhibition. *J Biol Chem* 274: 236–240, 1999.
31. **John S, Cesario D, Weiss JN.** Gap junctional hemichannels in the heart. *Acta Physiol Scand* 179: 23–31, 2003.
32. **Kang J, Kang N, Lovatt D, Torres A, Zhao Z, Lin J, Nedergaard M.** Connexin 43 hemichannels are permeable to ATP. *J Neurosci* 28: 4702–4711, 2008.
33. **Kanno S, Saffitz JE.** The role of myocardial gap junctions in electrical conduction and arrhythmogenesis. *Cardiovasc Pathol* 10: 169–177, 2001.
34. **Kondo RP, Wang SY, John SA, Weiss JN, Goldhaber JI.** Metabolic inhibition activates a non-selective current through connexin hemichannels in isolated ventricular myocytes. *J Mol Cell Cardiol* 32: 1859–1872, 2000.
35. **Leaphart CL, Dai S, Gribar SC, Richardson W, Ozolek J, Shi XH, Bruns JR, Branca M, Li J, Weisz OA, Sodhi C, Hackam DJ.** Interferon-gamma inhibits enterocyte migration by reversibly displacing connexin43 from lipid rafts. *Am J Physiol Gastrointest Liver Physiol* 295: G559–G569, 2008.
36. **Lewin E, Olgaard Klotho K.** An important new factor for the activity of Ca^{2+} channels, connecting calcium homeostasis, ageing and uraemia. *Nephrol Dial Transplant* 7: 1770–1772, 2006.
37. **Li H, Liu TF, Lazrak A, Peracchia C, Goldberg GS, Lampe PD, Johnson RG.** Properties and regulation of gap junctional hemichannels in the plasma membranes of cultured cells. *J Cell Biol* 134: 1019–1030, 1996.
38. **Li F, Sugishita K, Su Z, Ueda I, Barry WH.** Activation of connexin-43 hemichannels can elevate $[Ca^{2+}]_i$ and $[Na^+]_i$ in rabbit ventricular myocytes during metabolic inhibition. *J Mol Cell Cardiol* 33: 2145–2155, 2001.
39. **Majima HJ, Oberley TD, Furukawa K, Mattson MP, Yen HC, Szweda LI, St Clair DK.** Prevention of mitochondrial injury by manganese superoxide dismutase reveals a primary mechanism for alkaline-induced cell death. *J Biol Chem* 273: 8217–8224, 1998.
40. **Moore EW.** Ionized calcium in normal serum, ultrafiltrates, and whole blood determined by ion-exchange electrodes. *J Clin Invest* 49: 318–334, 1970.
41. **Morita M, Saruta C, Kozuka N, Okubo Y, Itakura M, Takahashi M, Kudo Y.** Dual regulation of astrocyte gap junction hemichannels by growth factors and a pro-inflammatory cytokine via the mitogen-activated protein kinase cascade. *Glia* 55: 508–515, 2007.
42. **Nazarov V, Aquino-DeJesus J, Apkon M.** Extracellular pH, Ca^{2+} influx, and response of vascular smooth muscle cells to 5-hydroxytryptamine. *Stroke* 31: 2500–2507, 2000.
43. **Neher E, Sakaba T.** Multiple roles of calcium ions in the regulation of neurotransmitter release. *Neuron* 59: 861–872, 2008.
44. **Orellana JA, Hernández DE, Ezan P, Velarde V, Bennett MV, Giaume C, Sáez JC.** Hypoxia in high glucose followed by reoxygenation in normal glucose reduces the viability of cortical astrocytes through increased permeability of connexin 43 hemichannels. *Glia* 58: 329–343, 2010.
45. **Palacios-Prado N, Sonntag S, Skeberdis VA, Willecke K, Bukauskas FF.** Gating, permselectivity and pH-dependent modulation of channels formed by connexin57, a major connexin of horizontal cells in the mouse retina. *J Physiol* 587: 3251–3269, 2009.
46. **Palacios-Prado N, Briggs SW, Skeberdis VA, Pranevicius M, Bennett MV, Bukauskas FF.** pH-dependent modulation of voltage gating in connexin45 homotypic and connexin45/connexin43 heterotypic gap junctions. *Proc Natl Acad Sci USA* 107: 9897–9902, 2010.
47. **Pearson RA, Dale N, Llaudet E, Mobbs P.** ATP released via gap junction hemichannels from the pigment epithelium regulates neural retinal progenitor proliferation. *Neuron* 46: 731–744, 2005.
48. **Pelegrin P, Surprenant A.** Pannexin-1 mediates large pore formation and interleukin-1β release by the ATP-gated $P2X_7$ receptor. *EMBO J* 25: 5071–5082, 2006.
49. **Peracchia C.** Chemical gating of gap junction channels; roles of calcium, pH and calmodulin. *Biochim Biophys Acta* 1662: 61–80, 2004.
50. **Plotkin LI, Manolagas SC, Bellido T.** Transduction of cell survival signals by connexin-43 hemichannels. *J Biol Chem* 277: 8648–8657, 2002.
51. **Rana S, Dringen R.** Gap junction hemichannel-mediated release of glutathione from cultured rat astrocytes. *Neurosci Lett* 415: 45–48, 2007.
52. **Retamal MA, Cortés CJ, Reuss L, Bennett MV, Sáez JC.** S-nitrosylation and permeation through connexin 43 hemichannels in astrocytes: induction by oxidant stress and reversal by reducing agents. *Proc Natl Acad Sci USA* 103: 4475–4480, 2006.
53. **Retamal MA, Schalper KA, Shoji KF, Bennett MV, Sáez JC.** Opening of connexin 43 hemichannels is increased by lowering intracellular redox potential. *Proc Natl Acad Sci USA* 104: 8322–8327, 2007.
54. **Retamal MA, Froger N, Palacios-Prado N, Ezan P, Sáez PJ, Sáez JC, Giaume C.** Cx43 hemichannels and gap junction channels in astrocytes are regulated oppositely by proinflammatory cytokines released from activated microglia. *J Neurosci* 27: 13781–13792, 2007.
55. **Ripps H, Qian H, Zakevicius J.** Properties of connexin26 hemichannels expressed in Xenopus oocytes. *Cell Mol Neurobiol* 24: 647–665, 2004.
56. **Rodrigues MA, Gomes DA, Andrade VA, Leite MF, Nathanson MH.** Insulin induces calcium signals in the nucleus of rat hepatocytes. *Hepatology* 48: 1621–1631, 2008.
57. **Romanello M, Pani B, Bicego M, D'Andrea P.** Mechanically induced ATP release from human osteoblastic cells. *Biochem Biophys Res Commun* 289: 1275–1281, 2001.
58. **Sánchez HA, Orellana JA, Verselis VK, Sáez JC.** Metabolic inhibition increases activity of connexin-32 hemichannels permeable to Ca^{2+} in transfected HeLa cells. *Am J Physiol Cell Physiol* 297: C665–C678, 2009.
59. **Silverman W, Locovei S, Dahl G.** Probenecid, a gout remedy, inhibits pannexin 1 channels. *Am J Physiol Cell Physiol* 295: C761–C767, 2008.
60. **Schalper KA, Palacios-Prado N, Retamal MA, Shoji KF, Martínez AD, Sáez JC.** Connexin hemichannel composition determines the FGF-1-induced membrane permeability and free $[Ca^{2+}]_i$ responses. *Mol Biol Cell* 19: 3501–3513, 2008.
61. **Schalper KA, Palacios-Prado N, Orellana JA, Sáez JC.** Currently used methods for identification and characterization of hemichannels. *Cell Commun Adhes* 15: 207–218, 2008.
62. **Schalper KA, Orellana JA, Berthoud VM, Sáez JC.** Dysfunctions of the diffusional membrane pathways mediated by hemichannels in inherited and acquired human diseases. *Curr Vasc Pharmacol* 7: 486–505, 2009.
63. **Schock SC, Leblanc D, Hakim AM, Thompson CS.** ATP release by way of connexin 36 hemichannels mediates ischemic tolerance in vitro. *Biochem Biophys Res Commun* 368: 138–144, 2008.
64. **Shestopalov VI, Panchin Y.** Pannexins and gap junction protein diversity. *Cell Mol Life Sci* 65: 376–394, 2008.
65. **Shintani-Ishida K, Uemura K, Yoshida K.** Hemichannels in cardiomyocytes open transiently during ischemia and contribute to reperfusion injury following brief ischemia. *Am J Physiol Heart Circ Physiol* 293: H1714–H1720, 2007.
66. **Sosinsky GE, Solan JL, Gaietta GM, Ngan L, Lee GJ, Mackey MR, Lampe PD.** The C-terminus of connexin43 adopts different conformations in the Golgi and gap junction as detected with structure-specific antibodies. *Biochem J* 408: 375–385, 2007.
67. **Stout C, Charles A.** Modulation of intercellular calcium signaling in astrocytes by extracellular calcium and magnesium. *Glia* 43: 265–273, 2003.
68. **Thimm J, Mechler A, Lin H, Rhee S, Lal R.** Calcium-dependent open/closed conformations and interfacial energy maps of reconstituted hemichannels. *J Biol Chem* 280: 10646–10654, 2005.
69. **Trexler EB, Bukauskas FF, Bennett MV, Bargiello TA, Verselis VK.** Rapid and direct effects of pH on connexins revealed by the connexin46 hemichannel preparation. *J Gen Physiol* 113: 721–742, 1999.
70. **Vergara L, Bao X, Cooper M, Bello-Reuss E, Reuss L.** Gap-junctional hemichannels are activated by ATP depletion in human renal proximal tubule cells. *J Membr Biol* 196: 173–184, 2003.
71. **Verma V, Hallett MB, Leybaert L, Martin PE, Evans WH.** Perturbing plasma membrane hemichannels attenuates calcium signalling in cardiac

cells and HeLa cells expressing connexins. *Eur J Cell Biol* 88: 79–90, 2009.

72. **Vinken M, Decrock E, De Vuyst E, De Bock M, Vandenbroucke RE, De Geest BG, Demeester J, Sanders NN, Vanhaecke T, Leybaert L, Rogiers V.** Connexin32 hemichannels contribute to the apoptotic-to-necrotic transition during Fas-mediated hepatocyte cell death. *Cell Mol Life Sci* 67: 907–918, 2009.
73. **Wakabayashi I, Groschner K.** Divergent effects of extracellular and intracellular alkalosis on Ca^{2+} entry pathways in vascular endothelial cells. *Biochem J* 323: 567–573, 1997.
74. **Wong CW, Christen T, Roth I, Chadjichristos CE, Derouette JP, Foglia BF, Chanson M, Goodenough DA, Kwak BR.** Connexin37 protects against atherosclerosis by regulating monocyte adhesion. *Nat Med* 12: 950–954, 2006.
75. **Ye ZC, Wyeth MS, Baltan-Tekkok S, Ransom BR.** Functional hemichannels in astrocytes: a novel mechanism of glutamate release. *J Neurosci* 23: 3588–3596, 2003.
76. **Yu J, Bippes CA, Hand GM, Muller DJ, Sosinsky GE.** Aminosulfonate modulated pH-induced conformational changes in connexin26 hemichannels. *J Biol Chem* 282: 8895–8904, 2007.